

Distance-Preserving Graph Embeddings from Random Neural Features

Daniele Zambon^{*1}, Cesare Alippi¹², and Lorenzo Livi³⁴

¹Università della Svizzera italiana, Lugano, Switzerland.

²Politecnico di Milano, Milano, Italy.

³University of Manitoba, Winnipeg, Canada.

⁴University of Exeter, Exeter, United Kingdom.

Abstract

We present Graph Random Neural Features (GRNF), a novel embedding method from graph-structured data to real vectors based on a family of graph neural networks. The embedding naturally deals with graph isomorphism and preserves, in probability, the metric structure of graph domain. In addition to being an explicit embedding method, it also allows to efficiently and effectively approximate graph metric distances (as well as complete kernel functions); a criterion to select the embedding dimension trading off the approximation accuracy with the computational cost is also provided. Derived GRNF can be used within traditional processing methods or as input layer of a larger graph neural network. The theoretical guarantees that accompany GRNF ensure that the considered graph distance is metric, hence allowing to distinguish any pair of non-isomorphic graphs.

1 Introduction

Inference on graph-structured data is one of the hottest topics in machine learning, thanks to successes achieved in several scientific fields, like neurosciences, chemistry, computational biology and social sciences [1–3]. One of the major research challenges there consists of building a practical solution able to process graphs, yet managing the graph isomorphism problem. A way to address this latter problem passes through metric distances and complete kernels, however, it has been shown to be at least as hard as deciding whether two graphs are isomorphic [4].

When data come as real vectors, the seminal paper by Rahimi and Recht [5] provides an efficient method to approximate radial basis kernels, exposing a parameter —the embedding dimension— trading off computational complexity with approximation error. The Random Kitchen Sinks [6] technique builds on [5] by adding a linear trainable layer and achieves, via convex optimization, an optimal estimation error on regression tasks [7]; see also [8, 9] for discussions. More recently, significant efforts aim at moving the research to the graph domain [10], with most of the contributions focusing on graph neural network properties, especially on their ability to discriminate between non-isomorphic graphs [11–13]. Recent research has also provided neural architectures granting the universal approximation property for functions on the graph domain [14, 15]; this holds asymptotically with the number of neurons.

Here we propose Graph Random Neural Features (GRNF), an embedding method that provides a map $\mathbf{z} : \mathcal{G} \rightarrow \mathbb{R}^M$ from attributed graphs to numeric vectors, and manages the graph isomorphism problem. We prove that GRNF is able to discriminate between any pair of non-isomorphic graphs in probability and preserves, approximately, the metric structure of the graph domain in the embedding space. Notably, GRNF can also be employed as the first layer of a graph neural network architecture. The main idea is to construct map \mathbf{z} from a family $\mathcal{F} = \{\psi(\cdot; \mathbf{w}) \mid \mathbf{w} \in \mathcal{W}\}$ of *graph neural feature* maps

^{*}Corresponding author, daniele.zambon@usi.ch.

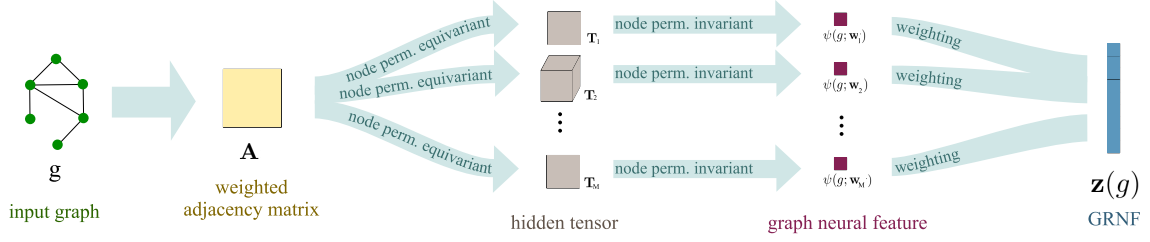


Figure 1: Scheme of a GRNF map $\mathbf{z} : \mathcal{G} \rightarrow \mathbb{R}^M$. A n -node graph $g \in \mathcal{G}$ is firstly represented as a weighted adjacency matrix $\mathbf{A} \in \mathcal{T}_n^2$ (Section 2). A collection of M graph neural features $\{\psi(g; \mathbf{w}_m)\}_{m=1}^M$ is then computed, weighted and, finally, concatenated in vector $\mathbf{z}(g)$. As described in Section 3, each graph neural feature map $\psi(\cdot; \mathbf{w}_m)$ is the composition of a node-permutation equivariant function, that maps matrix \mathbf{A} to a tensor $\mathbf{T}_m \in \mathcal{T}_n^k$ of (potentially different) order k , and a node-permutation invariant one, that maps \mathbf{T}_m to a scalar value $\psi(g; \mathbf{w}_m) \in \mathbb{R}$.

$\psi(\cdot; \mathbf{w}) : \mathcal{G} \rightarrow \mathbb{R}$, which are node-permutation-invariant graph neural networks with a single hidden-layer and a scalar output [16], and separates¹ graphs in \mathcal{G} . Parameter vector $\mathbf{w} \in \mathcal{W}$ is randomly sampled from a suitable distribution P and encodes the parameters associated with each neuron. Figure 1 provides a visual description.

The major theoretical contributions are associated with Theorems 1 and 2. In short,

- Theorem 1 shows that, given a suitable distribution P over parameter set \mathcal{W} , distance

$$d_P(g_1, g_2) = \sqrt{\mathbb{E}_{\mathbf{w} \sim P} [(\psi(g_1; \mathbf{w}) - \psi(g_2; \mathbf{w}))^2]}, \quad (1)$$

is metric. This implies that $d_P(g_1, g_2) > 0$ if and only if the two graphs are non-isomorphic.

- Theorem 2 proves that the squared distance $|\mathbf{z}(g_1) - \mathbf{z}(g_2)|_2^2$ between embedding vectors converges to $d_P(g_1, g_2)^2$ like $O(M^{-\frac{1}{2}})$, and constructively suggests an embedding dimension $M_{\epsilon, \delta}$ that guarantees the discrepancy between the two to be less than an arbitrary value ϵ with probability at least that $1 - \delta$. This guides the designer in selecting an embedding dimension M .

The paper is organized as follows. Section 3 introduces the family \mathcal{F} of graph neural features $\psi(\cdot; \mathbf{w})$. Section 4 defines distance d_P and proves Theorem 1. The GRNF map \mathbf{z} is presented in Section 5, where Theorem 2 is also proven. Section 6 relates our work with existing literature. Finally, experimental results in Section 7 empirically validate our theoretical developments.

2 Notation

For $k \in \mathbb{N}$, denote the space of order- k tensors with size n on every mode as

$$\mathcal{T}_n^k = \mathbb{R}^{\overbrace{n \times \dots \times n}^{k \text{ times}}},$$

and \mathbb{R} with \mathcal{T}_n^0 . Let us denote with $\pi \star \mathbf{T}$ the operation of applying permutation π , with π in the symmetric group S_n , to each mode of tensor $\mathbf{T} \in \mathcal{T}_n^k$, namely $(\pi \star \mathbf{T})_{i_1, \dots, i_k} = \mathbf{T}_{\pi(i_1), \dots, \pi(i_k)}$. In this paper we use the convention to represent with \mathbf{A} tensors of order 2, i.e., matrices, and with \mathbf{T} tensors of generic order $k \in \mathbb{N}_0$.

¹Family \mathcal{F} separates graphs of \mathcal{G} if for any pair of distinct (non-isomorphic) graphs $g_1, g_2 \in \mathcal{G}$, there exists a parameter vector $\mathbf{w} \in \mathcal{W}$ so that $\psi(g_1; \mathbf{w}) \neq \psi(g_2; \mathbf{w})$.

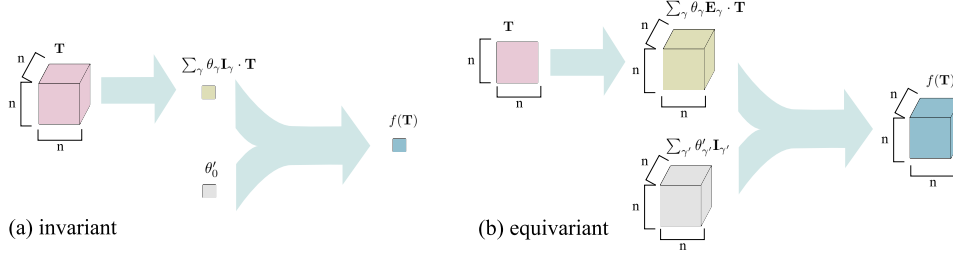


Figure 2: Structure of affine permutation invariant (a) and permutation equivariant (b) functions as linear combination of the bases $\{\mathbf{I}_\gamma\}$ and $\{\mathbf{E}_\gamma\}$ defined in Equation 2. In this example, $k = 3$.

Let us define a graph g with at most n nodes as a triple (V_g, E_g, at_g) , with $V_g \subseteq \{1, 2, \dots, n\}$ a set of nodes, $E_g \subset V_g \times V_g$ a set of edges, and attribute map $\text{at}_g : V_g \cup E_g \rightarrow \mathbb{R}$ associating nodes and edges with scalar attributes in a bounded subset of \mathbb{R} . We denote the set of such graphs with $\mathcal{G}(n)$, and with \mathcal{G} the space $\bigcup_{n \in \mathbb{N}} \mathcal{G}(n)$ of graphs with arbitrarily large, yet finite order. Under the assumption that no self-loops are present, we can represent each graph $g \in \mathcal{G}(n)$ with a tensor $\mathbf{A}_g \in \mathcal{T}_n^2$, where $(\mathbf{A}_g)_{i,i} = \text{at}_g(i)$, for $i \in V_g$, $(\mathbf{A}_g)_{i,j} = \text{at}_g((i,j))$, for $(i,j) \in E_g$ and $(\mathbf{A}_g)_{i,j} = 0$, otherwise. Different ordering choice of the nodes in V_g results in different representations \mathbf{A}_g . In our case, in which nodes are non-identified, this results in a bijection between $\mathcal{G}(n)$ and the quotient space $\mathcal{T}_{n/S_n}^2 = \{[\mathbf{A}]_{/S_n} \mid \mathbf{A} \in \mathcal{T}_n^k\}$ of equivalence classes $[\mathbf{A}]_{/S_n} = \{\pi \star \mathbf{A} \mid \pi \in S_n\}$.

3 Graph neural features

Given an integer $n \in \mathbb{N}$, we call *graph feature map* any function $f : \mathcal{T}_n^2 \rightarrow \mathbb{R}$ to the reals which is *invariant* under permutation of the nodes, namely, $f(\mathbf{A}_g) = f(\pi \star \mathbf{A}_g)$, for every $\pi \in S_n$; indeed, this is necessary to make $f(\mathbf{A}_g)$ a function of the graph g itself, and not of one of its representations $\mathbf{A} \in [\mathbf{A}_g]_{/S_n}$. For this reason, in the following we may use the notation $f(g)$ and $f(\mathbf{A}_g)$ interchangeably. Conversely, a function $f : \mathcal{T}_n^k \rightarrow \mathcal{T}_n^l$ is said *equivariant* to node permutation if $f(\pi \star \mathbf{T}) = \pi \star f(\mathbf{T})$, $\forall \pi \in S_n$.

Recent findings [16] have shown that the set of all linear permutation-invariant functions $\mathcal{T}_n^k \rightarrow \mathbb{R}$ is a vector space of dimension $\text{Bell}(k)$, i.e., the number of partitions of set $\{1, 2, \dots, k\}$; similarly, the space of linear permutation-equivariant functions is proven to be a $\text{Bell}(k+l)$ -dimensional vector space. Denoting with $\{\mathbf{I}_\gamma\}_{\gamma=1}^{\text{Bell}(k)}$ and $\{\mathbf{E}_\gamma\}_{\gamma=1}^{\text{Bell}(k+l)}$ the bases of invariant and equivariant linear spaces, respectively, we obtain that every affine invariant and equivariant function can be written in terms of tensor products and sums of the form

$$f(\mathbf{T}) = \begin{cases} H_k(\mathbf{T}; \boldsymbol{\theta}) = \sum_\gamma \theta_\gamma \mathbf{I}_\gamma \cdot \mathbf{T} + \theta'_0 & \text{if invariant} \\ F_{k,l}(\mathbf{T}; \boldsymbol{\theta}) = \sum_\gamma \theta_\gamma \mathbf{E}_\gamma \cdot \mathbf{T} + \sum_{\gamma'} \theta'_{\gamma'} \mathbf{I}_{\gamma'} & \text{if equivariant} \end{cases} \quad (2)$$

where $\{\theta_\gamma\}$ and $\{\theta'_{\gamma'}\}$ are coefficients that relates to the linear and bias parts, respectively, and $\boldsymbol{\theta} = \{\theta_\gamma\} \cup \{\theta'_{\gamma'}\}$. We refer the reader to Appendix A for a definition of $\{\mathbf{I}_\gamma\}$ and $\{\mathbf{E}_\gamma\}$, while Figure 2 provides a visual representation of these affine functions.

We are ready to define the set of graph neural features as composition of equivariant and invariant affine maps and some (nonlinear) activation functions.

Definition 1 (Graph neural feature). *We define graph neural feature a parametric map $\psi(\cdot; \mathbf{w}) : \mathcal{T}_n^2 \rightarrow \mathbb{R}$, with parameters $\mathbf{w} = (k, \boldsymbol{\theta}_F, \boldsymbol{\theta}_H)$, which results from the composition*

$$\mathcal{T}_n^2 \xrightarrow{F_{2,k}(\cdot; \boldsymbol{\theta}_F)} \mathcal{T}_n^k \xrightarrow{\rho_e} \mathcal{T}_n^k \xrightarrow{H_k(\cdot; \boldsymbol{\theta}_H)} \mathbb{R} \xrightarrow{\rho_i} \mathbb{R}$$

through activation functions ρ_i, ρ_e of an affine equivariant function $F_{2,k}(\cdot; \boldsymbol{\theta}_F)$ and an affine invariant one $H_k(\cdot; \boldsymbol{\theta}_H)$ in the form of (2), and with parameter space:

$$\mathcal{W} = \left\{ \mathbf{w} = (k, \boldsymbol{\theta}_F, \boldsymbol{\theta}_H) \quad \text{s.t.} \quad k \in \mathbb{N}, \quad \boldsymbol{\theta}_F \in \mathbb{R}^{\text{Bell}(k+2)+\text{Bell}(k)}, \quad \boldsymbol{\theta}_H \in \mathbb{R}^{\text{Bell}(k)+1} \right\}. \quad (3)$$

Notice that composing component-wise any activation function ρ_i, ρ_e to an affine invariant (equivariant) function gives an invariant (equivariant) function. Therefore, in the end $\psi(\cdot; \mathbf{w})$ is an invariant function. Without any ambiguity, we can write $\psi(g; \mathbf{w})$ as function of g . We stress since now that, despite ψ has been introduced for graphs in $\mathcal{G}(n)$, it is readily extended to operate on the entire space \mathcal{G} of finite-order graphs, because parameter space \mathcal{W} does not change with respect to n ; this is crucial to allow the comparison of graphs of different orders. We denote with

$$\mathcal{F}(\rho_i, \rho_e, \mathcal{W}), \quad (4)$$

or simply \mathcal{F} , the set of all graph neural feature maps defined over the entire \mathcal{G} .

As shown in the following Lemma 1, family \mathcal{F} separates graphs of \mathcal{G} , that is, it is rich enough to permit to distinguish between any pair of non-isomorphic graphs.

Lemma 1. *Let $\rho_e, \rho_i : \mathbb{R} \rightarrow \mathbb{R}$, with ρ_e squashing function, and ρ_i non-constant. Then set $\mathcal{F}(\rho_i, \rho_e, \mathcal{W})$ separates graphs of \mathcal{G} .*

The proof proceeds with the same strategy adopted by Hornik [17] to exhibit approximation capabilities of multi-layer perceptrons and, recently, by Keriven and Peyré [15] to graph neural networks; see Appendix B.1 for details.

4 A metric distance for graphs

The family \mathcal{F} of graph neural features (4) allows to define distance $d_P(g_1, g_2)$ in Equation 1 between two graphs $g_1, g_2 \in \mathcal{G}$, which assesses the expected discrepancy between graph neural features; this is possible whenever probability distribution P over \mathcal{W} is such that $\mathbb{E}_{\mathbf{w}}[\psi(g; \mathbf{w})^2] < \infty$ for every $g \in \mathcal{G}$. Notice that varying distribution P results in a different distance. In a supervised setting, this is a “parameter” that can be tuned (see subsequent Section 5), however, in general, we will see that one good choice is to take P such that its support $\text{supp}(P)$ is the entire set \mathcal{W} .

A simple example of distance d_P originates from considering a predefined set $\{\tilde{\mathbf{w}}_r\}_{r=1}^R$ of $R \in \mathbb{N}$ parameters and the uniform distribution over it. This specific choice gives

$$d_P(g_1, g_2) = \sqrt{\frac{1}{R} \sum_r (\psi(g_1; \tilde{\mathbf{w}}_r) - \psi(g_2; \tilde{\mathbf{w}}_r))^2},$$

and results in a pseudo-metric distance, because it is positive and symmetric, it satisfies the triangular inequality, but the *identifiability* property

$$\text{for any } g_1, g_2 \in \mathcal{G}, \quad g_1 = g_2 \iff d_P(g_1, g_2) = 0 \quad (5)$$

does not hold. It can be proved² that, regardless of the choice of P , the resulting distance d_P is always at least a pseudo-metric. Remarkably, a principled choice of P ensures that d_P is metric.

Theorem 1. *Consider set $\mathcal{F}(\rho_i, \rho_e, \mathcal{W})$ of graph neural features on graph set \mathcal{G} . Define a probability distribution P on \mathcal{W} , and the corresponding graph distance d_P like in (1). Under the following assumptions, space (\mathcal{G}, d_P) is metric.*

(A1) *Functions $\rho_i, \rho_e : \mathbb{R} \rightarrow \mathbb{R}$ are continuous, with ρ_e squashing function and ρ_i non-constant;*

²Please, see proof of Theorem 1.

(A2) Support $\text{supp}(P)$ of P covers \mathcal{W} ;

(A3) There exists a positive constant $C_{\mathcal{G}}$ such that the fourth momentum $\mathbb{E}_{\mathbf{w}}[\psi(g; \mathbf{w})^4] < C_{\mathcal{G}}$, for any choice of $g \in \mathcal{G}$; without loss on generality, we can assume $C_{\mathcal{G}} = 1$.

The core of the proof aims at showing that d_P possesses the identifiability property (5). To sketch the proof, notice that Assumption (A1) enables Lemma 1 and ensures that there exists a particular $\tilde{\mathbf{w}} \in \mathcal{W}$ for which $\psi(g_1; \tilde{\mathbf{w}}) \neq \psi(g_2; \tilde{\mathbf{w}})$. On the other hand, Assumption (A2) grants that every feature map in \mathcal{F} is taken into account by (1), and together with (A1), that we can find a neighbourhood $U(\tilde{\mathbf{w}})$ of non-null probability for which

$$\psi(g_1; \mathbf{w}) \neq \psi(g_2; \mathbf{w}), \quad \forall \mathbf{w} \in U(\tilde{\mathbf{w}}).$$

Property (5) eventually follows by the fact that $(\psi(g_1, \cdot) - \psi(g_2, \cdot))^2 \geq 0$.

Finally, showing that d_P is always positive, symmetric, and satisfies the triangular inequality is easier: observe that for every random variable X_1, X_2 , we have the Cauchy-Schwarz inequality $|\mathbb{E}[X_1 X_2]|^2 \leq \mathbb{E}[X_1^2] \mathbb{E}[X_2^2]$ and $\mathbb{E}[(X_1 + X_2)^2] \leq \mathbb{E}[X_1^2] + 2\sqrt{\mathbb{E}[X_1^2] \mathbb{E}[X_2^2]} + \mathbb{E}[X_2^2] = (\sqrt{\mathbb{E}[X_1^2]} + \sqrt{\mathbb{E}[X_2^2]})^2$. The triangular inequality follows from the choice $X_1 = \psi(g_1; \mathbf{w}) - \psi(g_3; \mathbf{w})$ and $X_2 = \psi(g_3; \mathbf{w}) - \psi(g_2; \mathbf{w})$. A detailed proof is provided in Appendix B.2.

Notice that Assumption (A3) is a convenient condition ensuring that every expected value is well-defined, and can be fulfilled by any bounded ρ_i . In general, all these assumptions result “only” in sufficient conditions, nevertheless, they are rather mild. One practical choice to satisfy them all is to build distribution P over a Poisson distribution to select the tensor order k and a corresponding multivariate Gaussian distribution for parameter vectors $\boldsymbol{\theta}_H, \boldsymbol{\theta}_F$, and to consider the sigmoid for both ρ_i and ρ_e .

Following the same rationale used for distance d_P , we define the following positive-definite kernel

$$\kappa_P(g_1, g_2) := \mathbb{E}_{\mathbf{w} \sim P} [\psi(g_1; \mathbf{w}) \psi(g_2; \mathbf{w})], \quad (6)$$

which is intimately related with d_P , in fact,

$$d_P(g_1, g_2)^2 = \kappa_P(g_1, g_1) - 2\kappa_P(g_1, g_2) + \kappa_P(g_2, g_2).$$

Further details about kernel κ_P are provided in Appendix C.1.

5 Graph random neural features

The definition of graph distance d_P in (1) as an expectation over the feature maps in \mathcal{F} allows us to create a random mapping that approximately preserves the metric structure of graph space (\mathcal{G}, d_P) .

Definition 2 (Graph Random Neural Features (GRNF)). *Given probability distribution P defined over \mathcal{W} and an embedding dimension $M \in \mathbb{N}$, we define Graph Random Neural Features map a function $\mathbf{z} : \mathcal{G} \rightarrow \mathbb{R}^M$ that associates to graph $g \in \mathcal{G}$ the vector*

$$\mathbf{z}(g; \mathbf{W}) := \frac{1}{\sqrt{M}} [\psi(g; \mathbf{w}_1), \dots, \psi(g; \mathbf{w}_M)]^\top, \quad (7)$$

where $\mathbf{W} = \{\mathbf{w}_m\}_{m=1}^M$ are drawn independently from P , and $\{\psi(\cdot; \mathbf{w}_m)\}_{m=1}^M \subseteq \mathcal{F}(\rho_i, \rho_e, \mathcal{W})$ are graph neural features (Definition 1).

When clear from the context, we may omit the explicit dependence from \mathbf{W} in $\mathbf{z}(g; \mathbf{W})$ and use the shorter form $\mathbf{z}(g)$. Figure 1 provides a visual representation.

Along the same lines of random Fourier features [5, 18] —but focusing on a distance rather than a kernel— we have that the squared norm $\|\mathbf{z}(g_1) - \mathbf{z}(g_2)\|_2^2$, which can be thought as a sample mean of

different graph neural features, is an unbiased estimator of the squared distance $d_P(g_1, g_2)^2$. Moreover, by the law of large numbers, we have the following convergence

$$|\mathbf{z}(g_1) - \mathbf{z}(g_2)|_2^2 \rightarrow d_P(g_1, g_2)^2, \text{ in probability as } M \rightarrow \infty. \quad (8)$$

Invoking the continuous-mapping theorem [19, Theo.2.3], we have also $|\mathbf{z}(g_1) - \mathbf{z}(g_2)|_2 \rightarrow d_P(g_1, g_2)$ in probability. The convergence (8) is of order \sqrt{M} , as one can see by

$$\text{Var} \left[|\mathbf{z}(g_1) - \mathbf{z}(g_2)|_2^2 \right] = \frac{1}{M^2} \sum_{m=1}^M \text{Var} \left[(\psi(g_1; \mathbf{w}) - \psi(g_2; \mathbf{w}))^2 \right] \quad (9)$$

$$\leq \frac{8}{M} (\mathbb{E} [\psi(g_1; \mathbf{w})^4] + \mathbb{E} [\psi(g_2; \mathbf{w})^4]) \stackrel{(\mathbf{A3})}{\leq} \frac{16}{M}, \quad (10)$$

thanks³ to the convexity of $g(x) = x^4$. Finally, exploiting the Chebyshev's inequality, the following theorem is proven.

Theorem 2. *Under Assumption (A3), for any value of $\varepsilon > 0$ and $\delta \in (0, 1)$, when $M \geq \frac{16}{\delta \varepsilon^2}$ we have*

$$\mathbb{P} \left(\left| |\mathbf{z}(g_1) - \mathbf{z}(g_2)|_2^2 - d_P(g_1, g_2)^2 \right| \geq \varepsilon \right) \leq \delta.$$

An analogous result is proven also for kernel κ_P :

$$\mathbf{z}(g_1)^\top \mathbf{z}(g_2) \rightarrow \kappa_P(g_1, g_2), \text{ in probability as } M \rightarrow \infty. \quad (11)$$

Remarkably, we can obtain the same convergence results also when sampling from a distribution \bar{P} different from P . It is only necessary to weight each component of map \mathbf{z} appropriately. In compliance with [18], we call *Weighted GRNF*

$$\bar{\mathbf{z}}(\cdot; \mathbf{W}) := \frac{1}{\sqrt{M}} \left[\dots, \sqrt{\frac{p(\mathbf{w}_m)}{\bar{p}(\mathbf{w}_k)}} \psi(\cdot; \mathbf{w}_m), \dots \right]^\top \quad (12)$$

where p and \bar{p} are the mixed-type probability distributions⁴ associated with P and \bar{P} , respectively. We refer the reader to Appendix C.2 for further details on this interesting setting.

The specific choice of distribution P induces different distances d_P (and kernel functions κ_P), and a principled choice of P can make the difference. In practice, we can exploit the trick of sampling from a predefined distribution \bar{P} , as in (12), and, a posteriori, identify a suitable distribution P that best serves the task to be solved [20]. Specifically, once M parameter vectors $\{\mathbf{w}_m\}_{m=1}^M$ are sampled from \bar{P} , we have that in (12) the scalars $\{p_m = p(\mathbf{w}_m)\}_{m=1}^M$ become free parameters.

6 Related work

The process of random sampling features takes inspiration from the work on random Fourier features [5]. There, shift-invariant kernels $\kappa(\mathbf{x}_1, \mathbf{x}_2) = \kappa(\mathbf{x}_1 - \mathbf{x}_2)$ are written in the form of an expected value

$$\mathbb{E}_{\omega \sim p} [\zeta(\mathbf{x}_1; \omega) \zeta(\mathbf{x}_2; \omega)^*] \quad (13)$$

with p being the Fourier transform of $\kappa(\cdot)$ and $\zeta(\mathbf{x}; \omega) = e^{i\omega^\top \mathbf{x}}$ (Bochner's theorem [21]). Random sampling parameters $\{\omega_m\}_{m=1}^M$ from p and $\{b_m\}_{m=1}^M$ from the uniform distribution $U([0, 2\pi))$, results in

$$\mathbb{E} \left[\frac{1}{M} \sum_m \cos(\omega_m^\top \mathbf{x}_1 + b_m) \cos(\omega_m^\top \mathbf{x}_2 + b_m) \right] = \kappa(\mathbf{x}_1, \mathbf{x}_2),$$

³Being x^p convex, we have $\left(\frac{X}{2} + \frac{Y}{2}\right)^p \leq \frac{X^p}{2} + \frac{Y^p}{2}$, therefore $\frac{1}{2^p} \mathbb{E}[(X+Y)^p] \leq \frac{1}{2}(\mathbb{E}[X^p] + \mathbb{E}[Y^p])$.

⁴We consider that random variable $\mathbf{w} = (k, \boldsymbol{\theta}_H, \boldsymbol{\theta}_F) \sim P$ is composed a discrete component k with probability mass function $p_k(k)$ and a continuous part $(\boldsymbol{\theta}_H, \boldsymbol{\theta}_F)$ with probability density function $p_\theta(\boldsymbol{\theta}_H, \boldsymbol{\theta}_F|k)$. Finally, we define with $p(\mathbf{w}) = p_k(k)p_\theta(\boldsymbol{\theta}_H, \boldsymbol{\theta}_F|k)$.

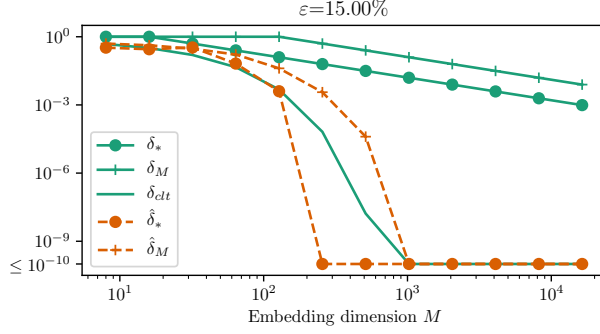


Figure 3: Empirical verification of Theorem 2. δ_M , δ_* and δ_{clt} defined as in Eq. 14, 15 and 16, respectively. $\hat{\delta}_M$ and $\hat{\delta}_*$ denote the empirical computation of the left-hand side in Eq. 14 and 15, respectively. Value of ε is set to the 15% of the squared graph distance computed with M_* .

hence providing a Monte Carlo approximation method. Clearly, being able to compute the Fourier transform p is crucial, however, it is not always possible; see, e.g., Vedaldi and Zisserman [22] for some examples. Extensions of this approach consider dot-product kernels $\kappa(\mathbf{x}_1, \mathbf{x}_2) = \kappa(\mathbf{x}_1^\top \mathbf{x}_2)$ [23]. The work by Yu et al. [24] proposed to keep an orthogonal structure in the matrix of sampled weights in order to achieve better approximations with a smaller number of features. We mention also the works by Wu et al. [25, 26] which, relying on a distance measure between data points, can apply the same rationale also to non-numeric data.

Our proposal builds on the framework of random features, but it works somehow in the opposite direction. Firstly, it defines a parametric family of features $\mathcal{F} = \{\psi(\cdot; \mathbf{w}) | \mathbf{w} \in \mathcal{W}\}$ that separates graphs of \mathcal{G} —playing the role of $\{\zeta(\cdot; \omega)\}$ in (13)— and, subsequently, it provides a distance (and kernel) function by selecting a probability distribution P on parameter space \mathcal{W} . This choice has the two major advantages: (1) it does not require to compute distribution P from a κ , and (2) allows the selection of the most appropriate distribution based on the task at hand.

7 Experimental validation

We provide empirical evidence of the validity of the bounds in Theorem 2. Since it is not always possible to compute the true value of d_P , we make use of two GRNF, $\mathbf{z}(\cdot; \mathbf{W}_1)$ and $\mathbf{z}(\cdot; \mathbf{W}_2)$, both with embedding dimension M . Calling $\Delta(\mathbf{W}) = |\mathbf{z}(g_1, \mathbf{W}) - \mathbf{z}(g_2, \mathbf{W})|_2^2$, we obtain⁵

$$\mathbb{P}(|\Delta(\mathbf{W}_1) - \Delta(\mathbf{W}_2)| \geq \varepsilon) \leq \frac{128}{M \varepsilon^2} =: \delta_M; \quad (14)$$

We also compared the above M -dimensional approximation Δ with a better estimate $\Delta_* := |\mathbf{z}_*(g_1) - \mathbf{z}_*(g_2)|_2^2$ based on a M_* -dimensional map \mathbf{z}_* with $M_* \gg M$. Assuming that equation $\Delta_* = d_P(g_1, g_2)^2$ holds

$$\mathbb{P}(|\Delta - \Delta_*| \geq \varepsilon) \leq \frac{16}{M \varepsilon^2} =: \delta_*. \quad (15)$$

Finally, we have performed a comparison with the estimate provided by the central limit theorem, i.e., assuming that the left-hand side in (15) is equal to

$$2\Phi\left(-\sqrt{M}\frac{\varepsilon}{\sigma}\right) =: \delta_{clt} \quad (16)$$

⁵ For any $\alpha \in (0, 1)$, it holds true that $\mathbb{P}(|A - B| \geq \varepsilon) \leq \mathbb{P}(|A - C| + |C - B| \geq \varepsilon) \leq \mathbb{P}(|A - C| \geq \varepsilon \alpha) + \mathbb{P}(|C - B| \geq \varepsilon(1 - \alpha))$. By substituting $\alpha = \frac{1}{2}$, $A = \Delta(\mathbf{W}_1)$, $B = \Delta(\mathbf{W}_2)$ and $C = d_P(g_1, g_2)^2$, we obtain (14).

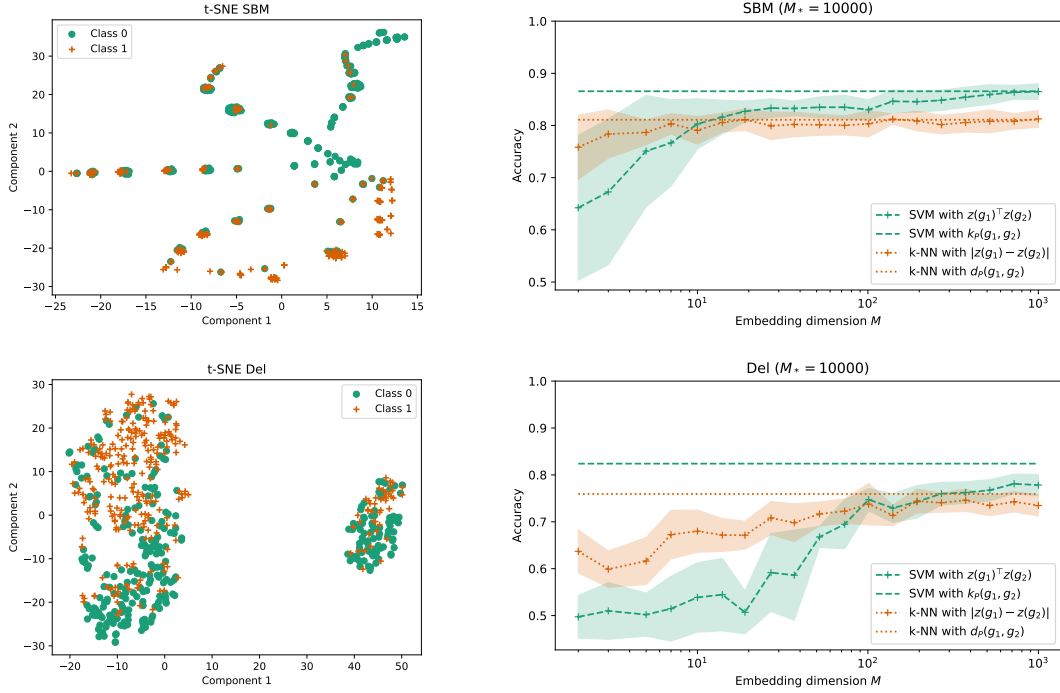


Figure 4: Left) 2-dimensional visualization of the embedding vectors $\mathbf{z}_*(g_i)$ for $i = 1, \dots, 600$ drawn with t-SNE. Right) Classification performance in terms of accuracy using different embedding dimensions M . First and second rows correspond to data sets SBM and Del, respectively. Each reported accuracy value is an average across 10 repetitions and the shaded region represents one standard deviation around the average.

where Φ is the cumulative density function of standard Gaussian distribution and $\sigma^2 = \text{Var}[(\psi(g_1; \mathbf{w}) - \psi(g_2; \mathbf{w}))^2]$. Results shown in Figure 3 confirm the theoretical predictions.

The second part of the experimental campaign is conducted by comparing the performance drop in adopting the approximations (11) and (8) with varying embedding dimension M . The task is binary classification, and it is performed using support vector machine and k-nearest neighbour classifiers, as standard kernel- and distance-based methods. We considered two data sets.

Graphs from the stochastic block model (SBM). We generated two classes of 300, 8-node graphs from the stochastic block model [27]. Class 0 has a single community with edge probability 0.4, while class 1 has two communities of 4 and 4 nodes with intra-community edge-probabilities of 0.8 and 0.6, respectively, and inter-community probability equal to 0.2.

Delaunay’s triangulation graphs (Del). We also tested on two classes of Delaunay’s triangulation graphs [28] with 300 6-node graphs per class. The graphs of a single class have been generated starting from a collection of 6 planar points, called seed points (the two classes are determined by different collections of seed points). The seed points are then perturbed with Gaussian noise. Each point corresponds to a node of the graph and its first coordinate is considered as node attribute. Finally, the Delaunay’s triangulation of the perturbed points gives the topology of the graph.

Figure 4 shows a t-SNE [29] visualization of the data sets and the achieved classification accuracy. We see that the accuracy obtained with GRNF empirically converges to the accuracy obtained with $M_* = 10^4$ features.

8 Conclusions

The present paper proposes a graph embedding method that we called Graph Random Neural Features (GRNF). The method preserves, with arbitrary precision, the metric structure of the graph domain. GRNF is based on a family $\mathcal{F} = \{\psi(\cdot; \mathbf{w}) : \mathcal{G} \rightarrow \mathbb{R}\}$ of graph neural networks, with parameter vector $\mathbf{w} \in \mathcal{W}$, that separates graphs of \mathcal{G} . By defining a probability distribution P over set \mathcal{W} , we can sample and weight M graph neural features to obtain the proposed GRNF map $\mathbf{z} : \mathcal{G} \rightarrow \mathbb{R}^M$.

Our results show that a distance for graphs can be obtained as the expectation of the squared discrepancy $(\psi(g_1; \mathbf{w}) - \psi(g_2; \mathbf{w}))^2$; similarly, $\mathbb{E}_{\mathbf{w}}[\psi(g_1; \mathbf{w})\psi(g_2; \mathbf{w})]$ leads to a positive-definite kernel function for graphs. Theorem 1 states that, when $\text{supp}(P) = \mathcal{W}$ the resulting graph distance is a metric: this implies that, in principle, it is possible to distinguish between any pair of non-isomorphic graphs. Secondly, Theorem 2 proves that the Euclidean distance $\|\mathbf{z}(g_1) - \mathbf{z}(g_2)\|_2$ between embedding vectors $\mathbf{z}(g_1), \mathbf{z}(g_2)$ converges to the actual graph distance $d_P(g_1, g_2)$, and provides a criterion to select an embedding dimension M ensuring to preserve the metric structure of the original graph domain up to a prescribed error and probability. Another advantage of GRNF is that it does not require a training phase; nonetheless, it is possible to search for a distribution P that best suits the data and task at hand.

GRNF, besides providing an explicit embedding method, can be used as first layer of a larger graph neural network. Finally, approximating graph distances and kernels, the method can also be used in distance- and similarity-based machine learning methods.

Acknowledgements

This research is funded by the Swiss National Science Foundation project 200021_172671: “ALPSFORT: A Learning graPH-baSeD framework FORe cybeR-physical sysTEms”. LL gratefully acknowledges partial support of the Canada Research Chairs program.

References

- [1] D. C. Elton, Z. Boukouvalas, M. D. Fuge, and P. W. Chung, “Deep learning for molecular design—a review of the state of the art,” *Molecular Systems Design & Engineering*, 2019.
- [2] P. W. Battaglia, J. B. Hamrick, V. Bapst, A. Sanchez-Gonzalez, V. Zambaldi, M. Malinowski, A. Tacchetti, D. Raposo, A. Santoro, R. Faulkner *et al.*, “Relational inductive biases, deep learning, and graph networks,” *arXiv preprint arXiv:1806.01261*, 2018.
- [3] A. Li, S. P. Cornelius, Y.-Y. Liu, L. Wang, and A.-L. Barabási, “The fundamental advantages of temporal networks,” *Science*, vol. 358, no. 6366, pp. 1042–1046, 2017.
- [4] T. Gärtner, P. Flach, and S. Wrobel, “On graph kernels: Hardness results and efficient alternatives,” in *Learning Theory and Kernel Machines*. Springer, 2003, pp. 129–143.
- [5] A. Rahimi and B. Recht, “Random features for large-scale kernel machines,” in *Advances in Neural Information Processing Systems*, 2008, pp. 1177–1184.
- [6] —, “Weighted sums of random kitchen sinks: Replacing minimization with randomization in learning,” in *Advances in Neural Information Processing Systems*, 2009, pp. 1313–1320.
- [7] —, “Uniform approximation of functions with random bases,” in *46th Annual Allerton Conference on Communication, Control, and Computing*. IEEE, 2008, pp. 555–561.
- [8] J. C. Principe and B. Chen, “Universal approximation with convex optimization: Gimmick or reality?[discussion forum],” *IEEE Computational Intelligence Magazine*, vol. 10, no. 2, pp. 68–77, 2015.

- [9] A. Rudi and L. Rosasco, “Generalization properties of learning with random features,” in *Advances in Neural Information Processing Systems*, 2017, pp. 3215–3225.
- [10] L. Oneto, N. Navarin, M. Donini, A. Sperduti, F. Aioli, and D. Anguita, “Measuring the expressivity of graph kernels through statistical learning theory,” *Neurocomputing*, vol. 268, pp. 4–16, 2017.
- [11] Z. Chen, S. Villar, L. Chen, and J. Bruna, “On the equivalence between graph isomorphism testing and function approximation with gnns,” *arXiv preprint arXiv:1905.12560*, 2019.
- [12] H. Maron, H. Ben-Hamu, H. Serviansky, and Y. Lipman, “Provably powerful graph networks,” *arXiv preprint arXiv:1905.11136*, 2019.
- [13] K. Xu, W. Hu, J. Leskovec, and S. Jegelka, “How powerful are graph neural networks?” in *International Conference on Learning Representations*, 2019. [Online]. Available: <https://openreview.net/forum?id=ryGs6iA5Km>
- [14] H. Maron, E. Fetaya, N. Segol, and Y. Lipman, “On the universality of invariant networks,” in *International Conference on Machine Learning*, 2019, pp. 4363–4371.
- [15] N. Keriven and G. Peyré, “Universal invariant and equivariant graph neural networks,” *arXiv preprint arXiv:1905.04943*, 2019.
- [16] H. Maron, H. Ben-Hamu, N. Shamir, and Y. Lipman, “Invariant and equivariant graph networks,” in *International Conference on Learning Representations*, 2019. [Online]. Available: <https://openreview.net/forum?id=Syx72jC9tm>
- [17] K. Hornik, M. Stinchcombe, and H. White, “Multilayer feedforward networks are universal approximators,” *Neural Networks*, vol. 2, no. 5, pp. 359–366, 1989.
- [18] Z. Li, J.-F. Ton, D. Oglic, and D. Sejdinovic, “Towards a unified analysis of random Fourier features,” in *International Conference on Machine Learning*, 2019, pp. 3905–3914.
- [19] A. W. Van der Vaart, *Asymptotic Statistics*. Cambridge University Press, 2000, vol. 3.
- [20] A. Sinha and J. C. Duchi, “Learning kernels with random features,” in *Advances in Neural Information Processing Systems*, 2016, pp. 1298–1306.
- [21] W. Rudin, *Functional Analysis*. McGraw-Hill, 1991.
- [22] A. Vedaldi and A. Zisserman, “Efficient additive kernels via explicit feature maps,” *IEEE Transactions on Pattern Analysis and Machine Intelligence*, vol. 34, no. 3, pp. 480–492, 2012.
- [23] P. Kar and H. Karnick, “Random feature maps for dot product kernels,” in *Artificial Intelligence and Statistics*, 2012, pp. 583–591.
- [24] F. X. Yu, A. T. Suresh, K. Choromanski, D. Holtmann-Rice, and S. Kumar, “Orthogonal random features,” in *Advances in Neural Information Processing Systems*, 2016, pp. 1975–1983.
- [25] L. Wu, I. E.-H. Yen, F. Xu, P. Ravikumar, and M. Witbrock, “D2ke: From distance to kernel and embedding,” *arXiv preprint arXiv:1802.04956*, 2018.
- [26] L. Wu, I. E.-H. Yen, Z. Zhang, K. Xu, L. Zhao, X. Peng, Y. Xia, and C. Aggarwal, “Scalable global alignment graph kernel using random features: From node embedding to graph embedding,” in *Proceedings of the 25th ACM SIGKDD International Conference on Knowledge Discovery & Data Mining*. ACM, 2019, pp. 1418–1428.
- [27] P. W. Holland, K. B. Laskey, and S. Leinhardt, “Stochastic blockmodels: First steps,” *Social Networks*, vol. 5, no. 2, pp. 109–137, 1983.

- [28] D. Zambon, L. Livi, and C. Alippi, “Detecting changes in sequences of attributed graphs,” in *IEEE Symposium Series on Computational Intelligence*, Nov. 2017, pp. 1–7.
- [29] L. Maaten and G. Hinton, “Visualizing data using t-SNE,” *Journal of Machine Learning Research*, vol. 9, no. Nov., pp. 2579–2605, 2008.
- [30] D. Sejdinovic, B. Sriperumbudur, A. Gretton, and K. Fukumizu, “Equivalence of distance-based and RKHS-based statistics in hypothesis testing,” *The Annals of Statistics*, pp. 2263–2291, 2013.

A Vector space of invariant and equivariant linear graph operators

Denote with $\Gamma(k)$ the set of all partitions of $\{1, \dots, k\}$. Bell’s number $\text{Bell}(k)$ represents the cardinality of $\Gamma(k)$. Given a partition $\gamma \in \Gamma(k)$, we say that multi-index $\mathbf{a} \in \{1, \dots, n\}^k$ *complies* with γ if, for any $i, j \in \{1, \dots, n\}$, we have that $\mathbf{a}_i = \mathbf{a}_j$ if and only if i, j belong to the same set in γ .

For every $\gamma \in \Gamma(k)$, tensor $\mathbf{I}_\gamma \in \mathcal{T}_n^k$ is defined as $(\mathbf{I}_\gamma)_{\mathbf{a}} = 1$ for any \mathbf{a} complying with γ , and 0 otherwise. With the scalar tensor product

$$\mathbf{I} \cdot \mathbf{T} := \sum_{\mathbf{a} \in \{1, \dots, n\}^k} \mathbf{I}_{\mathbf{a}} \mathbf{T}_{\mathbf{a}} \in \mathbb{R},$$

for any $\mathbf{I}, \mathbf{T} \in \mathcal{T}_n^k$. We obtain that basis $\{\mathbf{I}_\gamma\}_{\gamma \in \Gamma(k)}$ is orthogonal, because the locations in which the tensors are non-null are disjoint.

Similarly, for every $\gamma \in \Gamma(k+l)$, tensor $\mathbf{E}_\gamma \in \mathcal{T}_n^{k+l}$ is defined as $(\mathbf{E}_\gamma)_{\mathbf{a}} = 1$ for any \mathbf{a} complying with γ , and 0 otherwise. Here the tensor product $\mathbf{E} \cdot \mathbf{T}$ between $\mathbf{E} \in \mathcal{T}_n^{k+l}$ and $\mathbf{T} \in \mathcal{T}_n^k$ is defined as

$$\mathbf{E} \cdot \mathbf{T} := \sum_{\mathbf{b} \in \{1, \dots, n\}^l} \sum_{\mathbf{a} \in \{1, \dots, n\}^k} \mathbf{E}_{\mathbf{b}, \mathbf{a}} \mathbf{T}_{\mathbf{a}} \in \mathcal{T}_n^l.$$

Again, for different γ, γ' , the basis elements \mathbf{E}_γ and $\mathbf{E}_{\gamma'}$ are orthogonal.

We refer the reader to the original paper for a detailed description [16].

B Proofs

B.1 Proof of Lemma 1

The proof employs the functions f^\otimes in the form

$$f^\otimes(g) = \sum_{s=1}^S H_{\Sigma k_s} \left[\rho_e \left(F_{2, k_{s,1}}^{(s,1)}(\mathbf{A}_g; \boldsymbol{\theta}_{s,1}) \right) \otimes \dots \otimes \rho_e \left(F_{2, k_{s,T}}^{(s,T)}(\mathbf{A}_g; \boldsymbol{\theta}_{s,1}) \right); \boldsymbol{\theta}_H \right] + b$$

with functions $\{H_i^{(s)}\}$ and $\{F_{2,j}^{(s,t)}\}$ linear invariant and equivariant functions as defined in (2), but without the bias terms. We denote with $\mathcal{N}^\otimes(\rho_e)$ the set of such functions letting S, T vary in \mathbb{N} , $b \in \mathbb{R}$, and for any $(k_{1,1}, \boldsymbol{\theta}_{s,t}, \boldsymbol{\theta}_H) \in \mathcal{W}$. We also denote with $\mathcal{N}(\rho_e)$ the restriction of $\mathcal{N}^\otimes(\rho_e)$ to $T = 1$, which is contained in the closure under finite sums of set $\mathcal{F}(\text{id}, \rho_e)$, where $\text{id} : \mathbb{R} \rightarrow \mathbb{R}$ is the identity function.

1) Keriven and Peyré showed that $\mathcal{N}^\otimes(\sigma)$, with σ the sigmoid activation, separates \mathcal{G} [15, Lem.2] and that $\mathcal{N}(\rho_e)$ is dense in $\mathcal{N}^\otimes(\sigma)$ for any squashing function ρ_e [15, Lem.3]. Since $\mathcal{N}(\rho_e) \subseteq \mathcal{F}(\text{id}, \rho_e)$, then $\mathcal{F}(\text{id}, \rho_e, \mathcal{W})$ is dense on $\mathcal{N}^\otimes(\rho_e)$, and it derives that $\mathcal{F}(\text{id}, \rho_e, \mathcal{W})$ separates points of \mathcal{G} , as well. We conclude that for any pair of distinct graphs $g_1 \neq g_2$ in \mathcal{G} , there is a function $\hat{f} \in \mathcal{F}(\text{id}, \rho_e, \mathcal{W})$, such that $\hat{f}(g_1) \neq \hat{f}(g_2)$.

2) Notice that, for any $a, b \in \mathbb{R}$, $f_{a,b}(\cdot) := af(\cdot) + b \in \mathcal{F}(\text{id}, \rho_e, \mathcal{W})$, and when $a \neq 0$ we also have $f_{a,b}(g_1) \neq f_{a,b}(g_2)$; therefore, we can push $f_{a,b}(g_1)$ and $f_{a,b}(g_2)$ to any desired location. Let $\delta := \tilde{f}(g_2) - \tilde{f}(g_1) > 0$ and, without loss on generality, assume that $\rho_i(0) \neq \rho_i(1)$ (in fact, ρ_i is non-constant). With the choice $a = \frac{1}{\delta}$ and $b = -\frac{\tilde{f}(g_2)}{\delta}$, we obtain that $f_{a,b}(g_2) = 0$ and $f_{a,b}(g_1) = 1$ and $\rho_i(f_{a,b}(g_2)) \neq \rho_i(f_{a,b}(g_1))$, which proves that for any $g_1 \neq g_2$ there exists a function $f \in \mathcal{F}(\rho_i, \rho_e, \mathcal{W})$ such that $f(g_1) \neq f(g_2)$.

B.2 Proof of Theorem 1

1) Since the $\delta(g_1, g_2) := (\psi(g_1) - \psi(g_2))^2 \geq 0$, $\delta(g_1, g_2) = \delta(g_2, g_1)$ and $\delta(g_1, g_1) = 0$ for any $g_1, g_2 \in \mathcal{G}$, then the same properties hold also for $d_P(g_1, g_2) = \sqrt{\mathbb{E}[\delta(g_1, g_2)]}$.

2) The Cauchy-Schwarz inequality

$$|\mathbb{E}[X_1 X_2]|^2 \leq \mathbb{E}[X_1^2] \mathbb{E}[X_2^2], \quad (17)$$

holds for any pair of random variables X_1, X_2 ; in fact, notice that

$$0 \leq \frac{1}{2} \mathbb{E} \left[\left(\frac{X}{\sqrt{\mathbb{E}[X^2]}} - \frac{Y}{\sqrt{\mathbb{E}[Y^2]}} \right)^2 \right] = 1 - \mathbb{E} \left[\frac{X}{\sqrt{\mathbb{E}[X^2]}} \frac{Y}{\sqrt{\mathbb{E}[Y^2]}} \right];$$

3) By (17), we have

$$\mathbb{E}[(X_1 + X_2)^2] \leq \mathbb{E}[X_1^2] + 2\sqrt{\mathbb{E}[X_1^2]\mathbb{E}[X_2^2]} + \mathbb{E}[X_2^2] = \left(\sqrt{\mathbb{E}[X_1^2]} + \sqrt{\mathbb{E}[X_2^2]} \right)^2. \quad (18)$$

The triangular inequality follows from the choice $X_1 = \psi(g_1; \mathbf{w}) - \psi(g_3; \mathbf{w})$ and $X_2 = \psi(g_3; \mathbf{w}) - \psi(g_2; \mathbf{w})$.

4) Finally, the identifiability property (5) is proved by the following Lemma 2.

Lemma 2. *Under Assumptions (A1) and (A2), we have that for any pair of graphs $g_1, g_2 \in \mathcal{G}$*

$$g_1 = g_2 \iff d_P(g_1, g_2) = 0.$$

Proof. Denote with \mathcal{W}_k the parameter set \mathcal{W} in which the hidden tensor order is fixed to k .

1) Assumption (A1) enables Lemma 1, therefore for any pair $g_1, g_2 \in \mathcal{G}$ with $g_1 \neq g_2$ there exists a parameter configuration $\tilde{\mathbf{w}} \in \mathcal{W}$ so that $\psi(g_1, \tilde{\mathbf{w}}) \neq \psi(g_2, \tilde{\mathbf{w}})$.

2) Again from Assumption (A1), for any $k \in \mathbb{N}$, we have that $\psi(g; \cdot) : \mathcal{W} \rightarrow \mathbb{R}$ limited to \mathcal{W}_k , is continuous, as it is the composition of linear operators and continuous activations ρ_i, ρ_e . This holds in particular for \tilde{k} , the hidden tensor order associated with $\tilde{\mathbf{w}}$. Therefore, there is a neighbourhood $U_{g_1, g_2}(\tilde{\mathbf{w}})$ of $\tilde{\mathbf{w}}$ such that

$$|\psi(g_1, \mathbf{w}) - \psi(g_2, \mathbf{w})| \geq \frac{\varepsilon_{g_1, g_2}}{2}, \quad \forall \mathbf{w} \in U(\tilde{\mathbf{w}}),$$

with $\varepsilon_{g_1, g_2} = |\psi(g_1; \tilde{\mathbf{w}}) - \psi(g_2; \tilde{\mathbf{w}})| > 0$.

3) Assumption (A2) ensures that $\text{supp}(P) = \mathcal{W}$, and that $P(U_{g_1, g_2}(\tilde{\mathbf{w}}))$ is strictly positive, independently on the choice of graphs g_1, g_2 . We conclude that for any pair g_1, g_2 of distinct graphs,

$$d_P(g_1, g_2) \geq P(U_{g_1, g_2}(\tilde{\mathbf{w}})) \frac{\varepsilon_{g_1, g_2}}{2} > 0.$$

□

C Further results

C.1 A complete graph kernel from graph neural feature

In line with the definition of graph distance d_P , a positive definite graph kernel $\kappa_P : \mathcal{G} \times \mathcal{G} \rightarrow \mathbb{R}$ can be defined according to (6). Kernel κ_P is intimately related with d_P and it can be interpreted as induced by the squared distance d_P^2 :

$$\kappa_P(g_1, g_2) = \frac{1}{2} (d_P(g_1, \mathbf{0})^2 + d_P(g_2, \mathbf{0})^2 - d_P(g_1, g_2)^2),$$

with $\mathbf{0} \in \mathcal{G}$ being the null graph with no edge and zero as vertex attributes. Alternatively, we also have

$$d_P(g_1, g_2)^2 = \kappa_P(g_1, g_1) - 2\kappa_P(g_1, g_2) + \kappa_P(g_2, g_2).$$

Proposition 1 shows that κ_P is a *complete* kernel, meaning that the canonical embedding $\phi : \mathcal{G} \rightarrow \mathcal{H}$ to the reproducing kernel Hilbert space \mathcal{H} , and for which we can write $\kappa(g_1, g_2) = \langle \phi(g_1), \phi(g_2) \rangle_{\mathcal{H}}$, is injective [4], thus it maps distinct graphs to different points in \mathcal{H} .

Proposition 1. *Under Assumptions (A2)–(A3), we have the following results:*

- d_P is of negative type, i.e., for every $S \in \mathbb{N}$, any set of graphs $\{g_s\}_{s=1}^S$ and any set of scalars $\{c_s\}_{s=1}^S$, with $\sum_s c_s = 0$, we have

$$\sum_{i=1}^S \sum_{j=1}^S c_i c_j d_P(g_i, g_j) \leq 0;$$

- κ_P is a complete graph kernel.

Proof. 1) Let us start showing that kernel $\kappa_P(g_1, g_2)$ is positive definite. Defining $f(\mathbf{w}) = \sum_{i=1}^S c_i \psi(g_i; \mathbf{w})$, we have that

$$\sum_{i,j=1}^S c_i c_j \kappa_P(g_i, g_j) = \mathbb{E} \left[\sum_{i,j=1}^S c_i \psi(g_i; \mathbf{w}) c_j \psi(g_j; \mathbf{w}) \right] = \mathbb{E} [f(\mathbf{w})^2] \geq 0. \quad (19)$$

2) Since $\sum c_i = 0$, we obtain that d_P^2 is a semi-metric of negative type:

$$\begin{aligned} \sum_{i,j=1}^S c_i c_j d_P(g_i, g_j)^2 &= \sum_{i,j=1}^S c_i c_j (\kappa_P(g_i, g_i) - 2\kappa_P(g_i, g_j) + \kappa_P(g_j, g_j)) \\ &= 0 - 2 \sum_{i,j=1}^S c_i c_j \kappa_P(g_i, g_j) + 0 \stackrel{(\text{Eq. 19})}{\leq} 0. \end{aligned}$$

From Proposition 3 in [30] we have that $d_P = (d_P^2)^{\frac{1}{2}}$ is of negative type, as well.

3) Finally, being d_P^2 a semi-metric of negative type, by Proposition 14 in [30] we obtain that the distance induced kernel κ_P is complete. □

C.2 Limiting the order of the hidden tensor: Weighted GRNF

Allowing order k to grow indefinitely might result in an infeasible computation load. In the following section, we show how to cope with this problem by defining a d_P and κ_P over a distribution P , while sampling parameter \mathbf{w} from a different and more convenient one, \bar{P} .

Limiting k to be less or equal than k^* results in distance $d_P(\cdot, \cdot)$ which is not metric, in general, and one can build practical counterexamples. Consider a P with $\text{supp}(P) = \mathcal{W}$, and assume p to be the marginal probability mass function associated to k . Consider also a nonempty subset $\mathcal{K} \subseteq \mathbb{N}$ and define the probability function \bar{P} with marginal probability mass function

$$\bar{p}(k) = \frac{p(k)}{P(\mathcal{K})}, \quad k \in \mathcal{K}, \quad \text{and } 0 \text{ otherwise}$$

where $P(\mathcal{K})$ is the normalizing factor $\sum_{l \in \mathcal{K}} p(l)$. We obtain that approximating κ_P and d_P^2 by sampling the parameters \mathbf{w} from \bar{P} , and considering the following modified GRNF

$$\bar{\mathbf{z}}(\cdot; \mathbf{W}) := \sqrt{P(\mathcal{K})} \mathbf{z}(\cdot; \mathbf{W}), \quad (20)$$

yields a practical alternative, as shown in the following lemma. We call $\bar{\mathbf{z}}$ in (20) *bounded-order GRNF* to distinguish it from the *plain* GRNF (7).

Lemma 3. *Consider the bounded-order GRNF (20). If ρ_i is bounded by a constant C_{ρ_i} , then*

$$\begin{aligned} \mathbb{E} [\bar{\mathbf{z}}(g_1; \mathbf{W})^\top \bar{\mathbf{z}}(g_2; \mathbf{W})] & \begin{cases} \geq \kappa_P(g_1, g_2) - (1 - \mathbb{P}_p(\mathcal{K})) 4C_{\rho_i}^2 \\ \leq \kappa_P(g_1, g_2) \end{cases} \\ \mathbb{E} [|\bar{\mathbf{z}}(g_1; \mathbf{W}) - \bar{\mathbf{z}}(g_2; \mathbf{W})|_2^2] & \begin{cases} \geq d_P(g_1, g_2)^2 - (1 - \mathbb{P}_p(\mathcal{K})) 4C_{\rho_i}^2 \\ \leq d_P(g_1, g_2)^2. \end{cases} \end{aligned}$$

Proof. **1)** Let us start with a generic random variable X .

$$\begin{aligned} \mathbb{E}_{\bar{P}}[X] &= \sum_{k=1}^{\infty} \bar{p}(k) X = \sum_{k \in \mathcal{K}} \bar{p}(k) X = \frac{1}{\mathbb{P}_p(\mathcal{K})} \sum_{k \in \mathcal{K}} p(k) X = \frac{1}{\mathbb{P}_p(\mathcal{K})} \sum_{k=1}^{\infty} p(k) X - \sum_{k \notin \mathcal{K}} p(k) X \\ &= \frac{1}{\mathbb{P}_p(\mathcal{K})} \mathbb{E}_p[X] - \frac{1}{\mathbb{P}_p(\mathcal{K})} \sum_{k \notin \mathcal{K}} p(k) X. \end{aligned}$$

2) Substituting $X = (\mathbf{z}(g_1; \mathbf{w}) - \mathbf{z}(g_2; \mathbf{w}))^2$ and $X = \mathbf{z}(g_1; \mathbf{w})^\top \mathbf{z}(g_2; \mathbf{w})$, and then taking the expectation with respect to the joint \bar{P} , we get $\mathbb{E}_{\bar{P}}[X] \leq d_P(g_1, g_2)^2$ and $\mathbb{E}_{\bar{P}}[X] \leq \kappa_P(g_1, g_2)$, respectively. Finally, being ρ_i bounded by a constant C_{ρ_i} , we get $X \leq 4C_{\rho_i}^2$, hence the thesis. \square

We stress that, despite the hidden orders are sampled from the bounded-order distribution \bar{p} , the result relates to distance $d_P(\cdot, \cdot)$, which is with respect to the original distribution P with $\text{supp}(P) = \mathcal{W}$.

As we can see, completely avoiding certain hidden tensor orders k comes with the price of biased estimations, which does not ensure convergence in (11) and (8). One can obtain consistent approximations (11) and (8) while mitigating the computational and memory burden by selecting probability distribution \bar{P} , which down-weights large hidden-tensor orders maintaining $\text{supp}(\bar{P}) = \mathcal{W}$. We can also make a step further and let the entire distribution P vary. We result in the Weighted GRNF defined in (12). This type of embedding is a generalization of both the plain GRNF (7) and the bounded-order GRNF (20).

We prove that a generalized version of Theorem 2 that applies to the weighted GRNF.

Theorem 3. *Consider a distribution \bar{P} over \mathcal{W} , with $\text{supp}(\bar{P}) = \mathcal{W}$. If there exists a positive constant $\overline{C_G}$ such that the fourth momentum*

$$\mathbb{E}_{\mathbf{w} \sim \bar{P}} \left[\frac{p(\mathbf{w})^2}{\bar{p}(\mathbf{w})^2} \psi(g; \mathbf{w})^4 \right] < \overline{C_G}$$

for any choice of $g \in \mathcal{G}$, then for any value $\varepsilon > 0$ and $\delta \in (0, 1)$, when $M \geq \frac{16\overline{C_G}}{\delta\varepsilon^2}$ we have

$$\mathbb{P} \left(\left| |\bar{\mathbf{z}}(g_1) - \bar{\mathbf{z}}(g_2)|_2^2 - d_P(g_1, g_2)^2 \right| \geq \varepsilon \right) \leq \delta.$$

Proof. Following the rationale of the proof of Theorem 2, we prove that $\mathbb{E}[|\bar{\mathbf{z}}(g_1) - \bar{\mathbf{z}}(g_2)|_2^2] = d_P(g_1, g_2)^2$ and that $\mathbb{E}[|\bar{\mathbf{z}}(g_1) - \bar{\mathbf{z}}(g_2)|_2^2]$ scales as $O(M^{-1})$. Finally, we apply the Chebyshev's inequality.

1) Denote with $\Delta(\mathbf{w}) = |\psi(g_1; \mathbf{w}) - \psi(g_2; \mathbf{w})|_2^2$.

$$\begin{aligned} \mathbb{E}_{\bar{P}^M} \left[|\bar{\mathbf{z}}(g_1) - \bar{\mathbf{z}}(g_2)|_2^2 \right] &= \sum_{m=1}^M \mathbb{E}_{\bar{P}} \left[\frac{1}{M} \frac{p(\mathbf{w}_m)}{\bar{p}(\mathbf{w}_m)} \Delta(\mathbf{w}_m) \right] = \frac{1}{M} \sum_{m=1}^M \int_{\mathcal{W}} \frac{p(\mathbf{w})}{\bar{p}(\mathbf{w})} \Delta(\mathbf{w}) \, dP(\mathbf{w}) \\ &= \int_{\mathcal{W}} \bar{p}(\mathbf{w}) \frac{p(\mathbf{w})}{\bar{p}(\mathbf{w})} \Delta(\mathbf{w}) \, d\mathbf{w} = \mathbb{E}_P [\Delta(\mathbf{w})] = d_P(g_1, g_2)^2 \end{aligned}$$

This holds thanks to the fact that $\bar{p}(\mathbf{w}) \neq 0$ for every $\mathbf{w} \in \mathcal{W}$, otherwise we would end up with a result similar to Lemma 3.

2) The variance can be bound in the same manner of (10), obtaining

$$\text{Var} \left[|\bar{\mathbf{z}}(g_1) - \bar{\mathbf{z}}(g_2)|_2^2 \right] = \frac{1}{M} \text{Var} \left[\frac{p(\mathbf{w})}{\bar{p}(\mathbf{w})} (\psi(g_1; \mathbf{w}) - \psi(g_2; \mathbf{w}))^2 \right] \leq \frac{16 \overline{C_{\mathcal{G}}}}{M}$$

3) Chebyshev's inequality gives us the bound

$$\mathbb{P}_{\bar{P}^M} \left(\left| |\bar{\mathbf{z}}(g_1) - \bar{\mathbf{z}}(g_2)|_2^2 - d_P(g_1, g_2) \right| \geq \varepsilon \right) \leq \frac{16 \overline{C_{\mathcal{G}}}}{M \varepsilon^2}$$

from which the thesis follows. □